ACS APPLIED MATERIALS & INTERFACES

Research Article

www.acsami.org

# Magnetic Particles as Liquid Carriers in the Microfluidic Lab-in-Tube Approach To Detect Phase Change

Nicholas A. Blumenschein,[†] Daewoo Han,[†] Marco Caggioni,[‡] and Andrew J. Steckl*[,†]

[†]Nanoelectronics Laboratory, Department of Electrical Engineering and Computing Systems, University of Cincinnati, Cincinnati, Ohio 45221-0030, United States

[‡]Beckett Ridge Technical Center, Procter and Gamble Co., Cincinnati, Ohio 45069, United States

**ABSTRACT:** Magnetic beads (MBs) with ∼1.9 μm average diameter were used to transport specific microliter-scale volumes of liquids between adjacent reservoirs within a closed tube under the influence of a magnetic field. The tube's inner surface is coated with a hydrophobic layer, enabling the formation of a surface tension valve by inserting an air gap between reservoirs. This transfer process was implemented by keeping the MBs stationary with a fixed external magnet while the liquid reservoirs were translated by a computer-controlled syringe pump system. The magnet induces the aggregation of MBs in a loosely packed cluster (void volume ∼90-95%) against the tube's inner wall. The liquid trapped in the MB cluster is transported across the air gap between reservoirs. Fluorescence intensity from a dye placed in one reservoir is used to measure the volume of liquid transferred between reservoirs. The carry-over liquid volume is controlled by the mass of the MBs within the device. The typical volume of liquid carried by the MB cluster is ∼2 to 3 μL/mg of beads, allowing the use of small samples. This technique can be used to study the effect of small compositional variation on the properties of fluid mixtures. The feasibility of this "lab-in-tube" approach for binary phase diagram determination in a water−surfactant (C12E5) system was demonstrated.

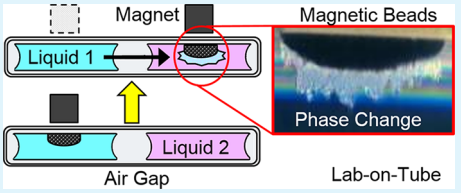


**KEYWORDS:** *magnetic beads, surface tension valve, lab-in-tube, fluorescence intensity, carry-over volume, surfactant*

## 1. INTRODUCTION

Magnetic beads (MBs) with micrometer and nanometer dimensions (generally referred to as "beads") in a fluidic environment have been used[1,2] for a variety of biomedical applications, such as cell separation, contrast agents, nucleic acid separation, drug targeting, and others. In most such applications, analysis based on MBs requires fairly complex microfluidic chips. An alternative approach uses magnetic beads to capture and transport biomolecules between individual liquid reservoirs located in a tube and isolated by air gaps. Although not as powerful as conventional microfluidic lab-on-chip devices, this lab-in-tube approach is much simpler to implement and operate, while still benefiting from the use of microliter-scale samples. The MB-based lab-in-tube has been recently reported[3] by Haselton's group and applied to low-cost nucleic acid assays.

A critical component of the lab-in-tube device is the design and operation of the surface-tension-controlled air valve that separates fluid compartments. Biomolecules attached to MBs are transported through air valves between fluid reservoirs under the influence of an external magnet. Because of the geometry of the magnet and the tube and the location of the MBs, an inhomogeneous magnetic field is produced, leading to a loose ("porous") clustering of the MBs against the tube wall. Fluid can penetrate the MB cluster, and a certain amount is transported from one reservoir to the next. In conventional biomedical analysis, this is undesirable, and design criteria for minimizing this carry-over fluid volume have been reported.[4] However, as seen below, in certain applications this effect can be beneficially utilized.

In this work, a report is presented on the use of the lab-in-tube approach for investigating phase diagrams of multi-component systems. Surfactant and microemulsion technologies play an important role in areas such as detergency,[5] oil recovery,[6] and drug delivery.[7] The optimization of the formulation and processes in these different areas relies on accurate characterization of the phase behavior of surfactant mixtures.[8] The development of reliable and convenient methods to map the equilibrium properties of phase diagram as well as the kinetics associated with the phase transition[9] remains an important area. Most of the practiced techniques for phase diagram investigation are currently based on preparing multiple samples with different compositions, ensuring that each sample reaches thermodynamic equilibrium and characterizing the phase(s) obtained. Most of these techniques involve a lengthy process and utilize a significant amount of material. For high-resolution phase diagram characterization, the diffusive interfacial transport (DIT) method has received considerable attention.[10,11] The DIT method uses a flat capillary and polarized light to image phase boundaries. For aqueous surfactant−solvent binary systems, infrared analysis is used to determine the water composition. The infrared analysis method has advantages in terms of sample quantity required, speed of

Received: January 4, 2014
Accepted: May 14, 2014
Published: May 14, 2014

   dx.doi.org/10.1021/am502845p | ACS Appl. Mater. Interfaces 2014, 6, 8066−8072

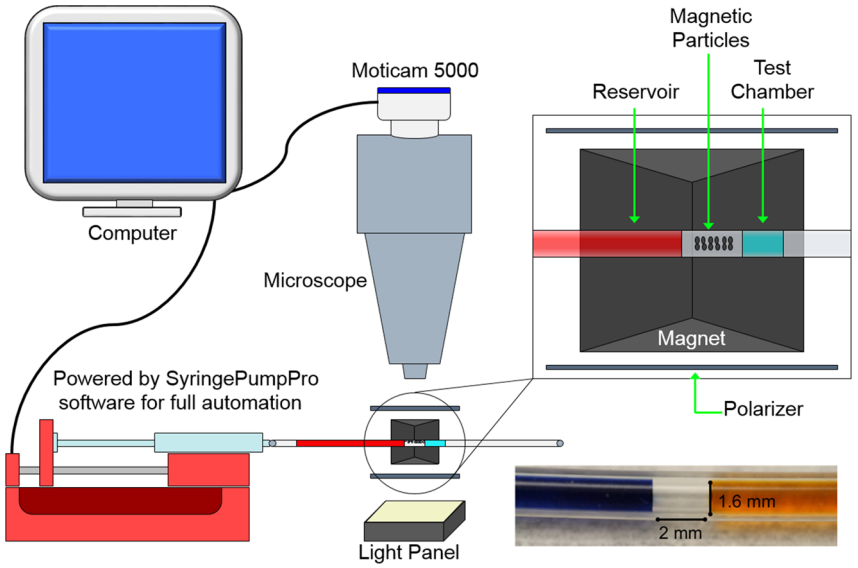


**Figure 1.** Schematic diagram of experimental setup. Inset: a photograph of the tube used in experiments, showing two liquid segments (water with blue fluorescent dye and ethanol with orange fluorescent dye) separated by an air valve.

experimental execution, and resolution. However, this method is not widely used, primarily because of the need for a significant initial capital investment.

Microfluidic chips have been utilized for exploring the phase diagrams of surfactant−water systems[12] and polymer−salt systems,[13] among others. As in the case of biomedical assays, the microfluidic chips are relatively complicated to design and operate. We report a simpler approach using the lab-in-tube approach to investigate the phase diagram of various materials by taking advantage of the carry-over liquid that accompanies the transport of MBs between reservoirs. The lab-in-tube approach also has the advantages of much smaller sample volume and resulting faster sample equilibration time.

The combination of water, surfactants, and organic solvents is found in many industrial applications, such as pharmaceuticals, biochemicals, food, cosmetics, and others. Precise knowledge of the related phase diagram under various conditions is very important for optimizing formulations, but it can be quite time consuming and require large sample volumes.

An important subset of phase diagrams is the case where the phase transition generates a new phase that has a much higher viscosity or, more generally, much different rheological properties. This type of phase change has been the object of much study because of the many challenges it poses from an industrial point of view. The specific two-component system of water and the non-ionic surfactant C12E5 (pentaethylene glycol monodecyl ether) was investigated using the lab-in-tube approach, as it represents a class of materials widely used in industry, for example, in detergent products. The $H_2O$−C12E5 phase diagram is very feature-rich. Transitions to liquid crystalline phases can be observed as a function of surfactant concentration and temperature, displaying many distinct phases.[14,15]

## 2. EXPERIMENTAL DETAILS

**2.1. Materials.** MB dispersions (AccuBead) were purchased from Bioneer Inc. (Alameda, CA). The composition of AccuBeads consists of 80 wt % iron oxide ($Fe_3O_4$) core with 20 wt % silica shell. The silica coating ensures compatibility of MBs with aqueous solutions. Typical dispersions used 1 g of magnetic beads in 50 mL of aqueous solutions. The C12E5 surfactant with 98% purity (Sigma-Aldrich, St. Louis, MO) was used as-received without further purification. Aqueous solution used was deionized water. Thermo Scientific Nalgene 890 tubing with an inner diameter of 1.6 mm and an outer diameter of 3.2 mm was used (Fisher Scientific, Pittsburgh, PA). The magnet used was a 1 inch cube (Apex Magnets, Petersburg, WV) made of neodymium of grade N48 with a pull force of 45.6 kg. Polarizer film (Edmund Optics, Barrington, NJ) had a thickness of 0.8 mm and a polarization efficiency of >99%. For hydrophobic coating on tube walls, Teflon AF solution (no. 400S1-100-1, Dupont, Wilmington, DE) was utilized. Keyacid Red dye with emission at 598 nm (Keystone, Chicago, IL) was used. The filter cube of a Nikon inverted microscope had an excitation wavelength range from 540−580 nm, with a dichroic mirror at 585 nm, allowing photoemission over the range of 593−668 nm.

**2.2. Sample Preparation.** Approximately 15 cm of tubing is used for each device. The tubing is prepared by coating the inner wall with Teflon AF (amorphous fluoropolymer) solution in order to increase the contact angle of the various liquids. This procedure was performed by injecting the Teflon solution into the tubing and allowing it to dry at room temperature for 1 h in air followed by heating in an oven at 100 °C for 1 h. Because the surface tension air valve is an integral element of the device, Teflon coating of the tube is required. Interaction between the Teflon coating and the fluids investigated (water and C12E5 surfactant) is likely to be minimal. This possibility will, however, be investigated in the future. In the experimental process, various concentrations of the MB dispersions were prepared by diluting original MB dispersions with deionized water.

**2.3. Methods.** The experimental setup is illustrated in Figure 1. To characterize the liquid transfer attributes of the magnetic beads, a tube is filled with two liquid segments of certain volumes/compositions separated by an air gap, which functions as a valve and keeps the two liquids separated. One liquid is preloaded with a mass of magnetic beads, and the second liquid (typically $H_2O$) contains a fluorescent dye. These two volumes of liquid are referred to as the test chamber and reservoir, respectively. Liquids, with typical reservoir and test chamber volumes of 180 and 20 $\mu$L, are inserted into the tubing using a Stoelting 53130 syringe pump. With the tube device prepared, initial measurements of the color intensity of each volume are taken using a Nikon Eclipse Ti inverted microscope: $I_{R0}$, initial reservoir intensity; $I_{T0}$, initial test chamber intensity. Next, the mixing of the two liquids using the magnetic beads is initiated. The magnetic beads form a cluster against the inner wall of the tubing because of the external magnet, trapping a carry-over liquid volume within the cluster. Using the magnet to hold the MBs stationary while the liquid reservoirs are

translated by the syringe pump, the magnetic beads are transferred from the reservoir containing the fluorescent dye, through the air gap, and into the test chamber, which is initially dye-free. This approach of keeping the MBs stationary while the fluids are transported is the reverse of that of Bordelon et al.[3] and is selected in order to minimize variations in MB aggregation configuration during each transfer and related changes in carry-over volume. Once the test chamber is reached, a mixing process is performed to evenly disperse this fluorescent liquid into the clear liquid, making the entirety of the volume homogenous in fluorescence intensity. After every transfer, the fluorescence intensity of the reservoir ($I_{Rn}$) and the test chamber ($I_{Tn}$) is measured. After all transfer cycles are completed, the liquids in the test and reservoir chambers are removed from the tube into a dish, where liquids surrounding the MBs evaporate, allowing for the measurement of the mass of MBs using the Denver Instruments PI-225D balance with a measurement accuracy of 10 $\mu$g. Measurements were also carried out to determine the amount of MBs remaining in one chamber while the cluster is crossing the air valve to the second chamber. It was determined that this number is less than 10 $\mu$g (the accuracy of the balance) versus a total MB mass of 500−800 $\mu$g. Therefore, it is concluded that the transport process carries nearly 100% of the MBs.

**2.4. Numerical Analysis Using MATLAB.** A simple (linear) relationship was developed between the fluorescence intensity of the reservoir and test chambers (after each transfer) and the carry-over volume. This relationship was used in MATLAB to extract values for the carry-over volume by curve fitting the output of the simulation to experimental results. Equations 1 and 2 simulate the fluorescence intensity in the reservoir and test chambers after $n$ transfers

$$I_{Rn} = \frac{I_{R(n-1)} \times (V_R - V_C) + (I_{Tn} \times V_C)}{V_R} \quad (1)$$

$$I_{T(n+1)} = \frac{(I_{Tn} \times V_T) + (I_{Rn} \times V_C)}{V_T + V_C} \quad (2)$$

where $I_{Rn}$ is the fluorescence intensity of the reservoir at $n$ transfers, $I_{T(n+1)}$ is the fluorescence intensity of the test chamber at $n + 1$ transfers, $V_R$ and $V_T$ are the initial reservoir and initial test chamber volumes, respectively, and $V_C$ is the carry-over volume.

Obtaining a good approximation of the carry-over volume as a function of the mass (or number) of magnetic beads is very useful for carrying out future experiments without the need of the fluorescent dye and for designing related devices for various applications.

## 3. RESULTS AND DISCUSSION

Figure 2 shows scanning electron microscope (SEM) images of the MBs and a histogram of MB diameters. The MBs ranged in diameter from 1 to 8 $\mu$m, with an average value of 1.9 $\mu$m and a standard deviation of 1.2 $\mu$m. On the basis of the 80:20 weight distribution between the iron oxide core and silica sheath, the average core diameter is 1.67 $\mu$m, whereas the average sheath thickness is 95 nm.

The transport of the MB cluster from the water reservoir into the air gap is illustrated in the photographs in Figure 3. As can be seen from both the top view and side view of the cluster, its volume is reduced significantly (by a factor of ∼3) as it transitions from water to air. This effect is caused by the water surface tension at the interface between water and air. This effect is dramatically illustrated in the fourth photographs of each column in Figure 3, where water from within the cluster is observed being pulled back into the reservoir even as the cluster is fully located within the air gap. The approximate porosity (based on calculated volume of the MB mass) of the cluster in water is 90−95%, whereas in the air gap it is 80−85%.

Initial experiments compared the use of the porous MB cluster with a solid magnetic stir bar. Figure 4 compares the

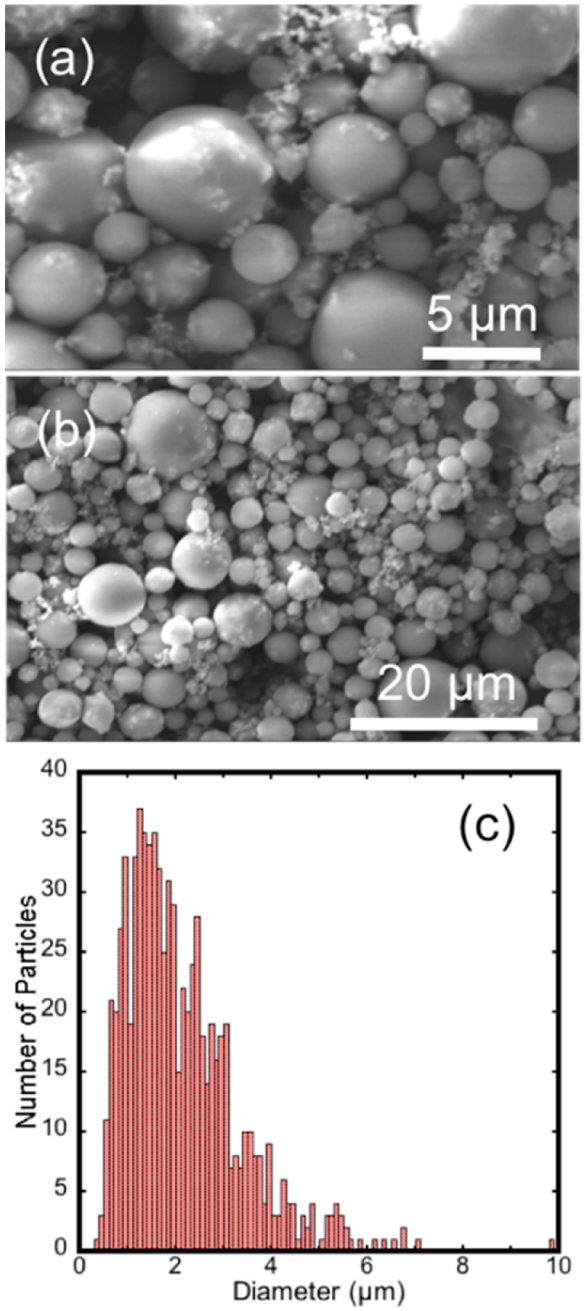


**Figure 2.** Magnetic beads used in this study: (a) SEM photomicrograph at 5000×, (b) SEM photomicrograph at 2000×, and (c) histogram plot of MB size distribution (no. of beads vs diameter). The diameter range was from ∼1 to 10 $\mu$m, with a median diameter of 1.9 $\mu$m and standard deviation of 1.2 $\mu$m.

fluorescence intensity in the test chamber of each device (MBs, stir bar) as a function of the number of transfers. For each case, the devices contained a 180 $\mu$L reservoir, a 20 $\mu$L test chamber, and a 6 $\mu$L air gap. Given that the fluorescence intensity increases more rapidly in the case of AccuBeads, it is concluded that they transport a larger carry-over volume. The mass of the magnetic bar was the same as that of the magnetic bead cluster (∼0.5 mg). The range in carry-over volume for the AccuBeads is calculated to be 1.2−1.4 $\mu$L, as compared to 0.1−0.2 $\mu$L for the stir bar. It is clear that the stir bar was significantly less effective than the magnetic beads.


dx.doi.org/10.1021/am502845p | ACS Appl. Mater. Interfaces 2014, 6, 8066−8072

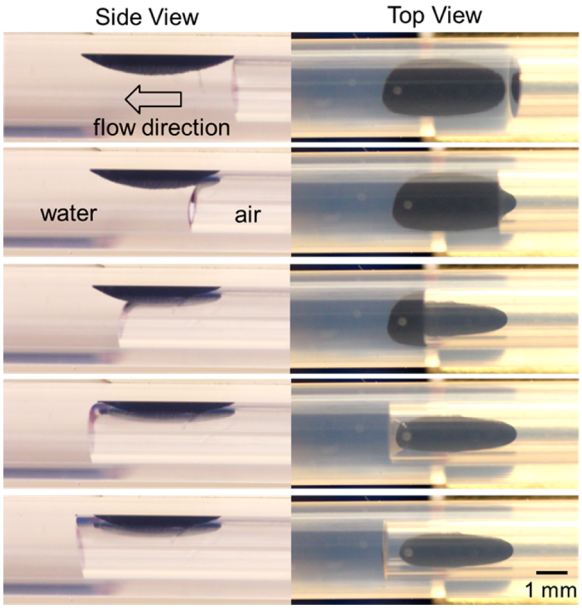


**Figure 3.** Magnetic bead cluster (AccuBeads) held in place while the water reservoir is being pumped from right to left. Left column shows the side view of cluster, and the right column shows a top view.

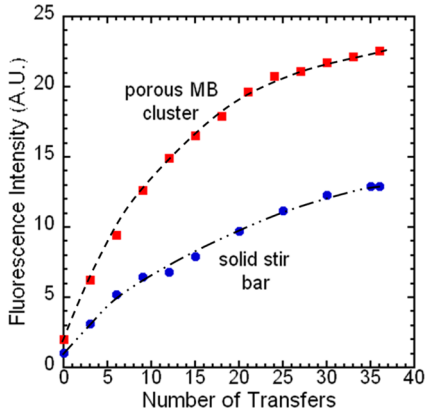


**Figure 4.** Fluorescence intensity in the test chamber as a function of number of transfers for magnetic beads and a magnetic stir bar with the same mass of ~0.5 mg.

The effect of relative size between the reservoir and test chamber volume was investigated in order to be able to control the relative amount of liquid being transferred between the two reservoirs. This is important in the application of this technique to phase diagram investigation, as certain amounts of water and surfactant lead to phase change. Two devices were made containing a similar MB mass (~0.6 mg), the same reservoir volume of 180 $\mu$L, and separated by an air gap of 6 $\mu$L but with test chamber volumes of 20 and 40 $\mu$L. To keep the MB amount the same in both devices, the device with the 20 $\mu$L test chamber used a 40% concentration of the MB solution, whereas the device with the 40 $\mu$L test chamber used a MB concentration of 20%.

The results are shown in Figure 5. As expected, for a smaller test chamber, a larger change in the fluorescence intensity is observed as a function of number of transfers. For the 20 $\mu$L test chamber, the fluorescence intensity reaches a saturation value of ~22 a.u. after ~95 transfers, whereas for the 40 $\mu$L test chamber, the saturation value (~21 a.u.) is reached after ~160

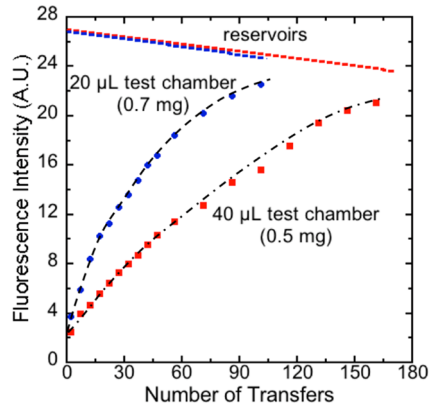


**Figure 5.** Fluorescence intensity as a function of number of transfers for two devices with the same reservoir volume (180 $\mu$L) and different test chamber volumes (20 and 40 $\mu$L) with approximately the same mass of MBs.

transfers. The difference in the number of transfers to reach saturation for the two test chambers is related to the point at which the saturation concentration is reached in their respective volume. As seen in Figure 5, the saturation concentration in the two test chambers is nearly identical. At the same time, the fluorescence intensity in the reservoir chambers decreases with increasing numbers of transfers because of a corresponding reduction in dye concentration. A similar convergence between the fluorescence signal intensity from the reservoir and test chambers is observed in both cases. Complete convergence is expected for a larger number of transfers.

Next, the effect of the number of magnetic beads (total bead mass) on the fluid transfer efficiency was investigated. The experiment compared several magnetic bead concentrations placed within the test chamber in three separate devices. Each device had reservoir and test volumes of 180 and 20 $\mu$L, respectively, and an air gap volume of 6 $\mu$L. The MB solution was diluted with water to produce solutions with varying MB content of 0.24, 0.4, and 0.48 mg, respectively. The effect of MB mass on the fluorescence intensity of the test chamber as a function of the number of transfer is illustrated in Figure 6. Because the fluorescence intensity in the test chamber is a function of the cumulative amount of dye that is transferred by the MBs, this provides a method for determining the carry-over liquid volume for different number of MBs. The curves shown

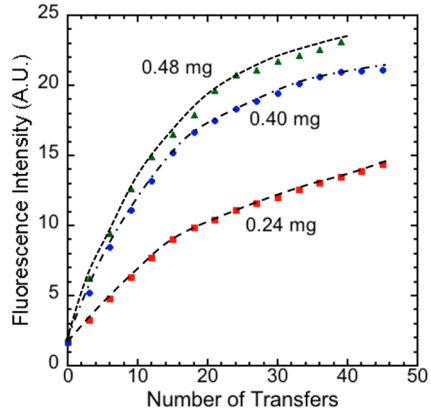


**Figure 6.** Fluorescence intensity in the test chamber as a function of number of transfers for three concentrations of 1.9 $\mu$m beads sizes: ~0.24, 0.4, and 0.48 mg.


dx.doi.org/10.1021/am502845p | ACS Appl. Mater. Interfaces 2014, 6, 8066−8072

in Figure 6 confirm that the carry-over volume increases with MB mass.

Using the average fluorescence intensity change over the entire number of transfers as a yardstick for comparison, the 0.24 mg MB solution produced an intensity change of 28.3 a.u. per transfer and a carry-over volume ranging from 0.32−0.45 $\mu$L, whereas the 0.40 and 0.48 mg solutions resulted in 43.1 and 54.1 a.u. intensity change per transfer (with carry-over volumes ranging from 0.7−1.05 $\mu$L and 1.2−1.4 $\mu$L), respectively. Using the MATLAB analytical simulation described in Section 2.4, the fluorescence intensity change for each device is converted into carry-over volume, shown in Figure 7. The two different values of the carry-over volume shown for each mass of MBs come from the best upper bound and lower bound curve fitting numerical solutions obtained from the MATLAB analysis.

The results in Figure 7 clearly indicate that one can control the volume of transferred fluids between isolated reservoirs by adjusting the total MB mass. In turn, this will enable the efficient exploration of the phase diagram space in increments selected to provide high resolution in the vicinity of phase change regions and lower resolution elsewhere.

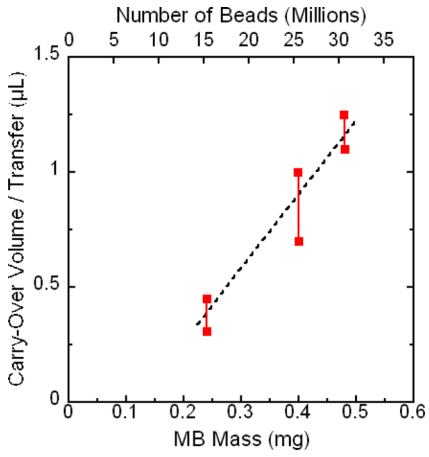


**Figure 7.** Average carry-over liquid volume per transfer as a function of MB mass.

The carry-over liquid volumes are shown in Figure 7 for three MB clusters (0.24, 0.40, and 0.48 mg). The carry-over volume is seen to increase linearly with MB mass, ranging from an average of 0.4 $\mu$L for the 0.24 mg cluster to an average of 1.3 $\mu$L for the 0.48 mg cluster. An extrapolated carry-over volume of ~2.8 $\mu$L is calculated for a 1 mg MB cluster. These carry-over volumes are comparable to those reported in other studies. For example, Adams et al. have reported[4] a carry-over volume of ~1.5 $\mu$L/mg for beads with 1.15 $\mu$m diameter (Dynabeads MyOne Silane beads). This carry-over volume is approximately half of what is reported here. This difference in carry-over volume is probably related to the tighter packing of the AccuBeads cluster resulting from a wide range of bead diameters, with smaller beads filling in the gaps between larger beads, thus trapping the liquid in the bead cluster more effectively as it is transported through the air valve. In contrast, the Dynabeads have a uniform diameter distribution that leads to less dense packing, which in turn may allow fluid to escape more readily.

The feasibility of using MB-based liquid transport for studying the phase diagrams of multicomponent systems was investigated using the combination of water and the surfactant C12E5. The $H_2O$−C12E5 phase diagram shown in Figure 8b (modified from Hishida and Tanaka[14]) contains multiple

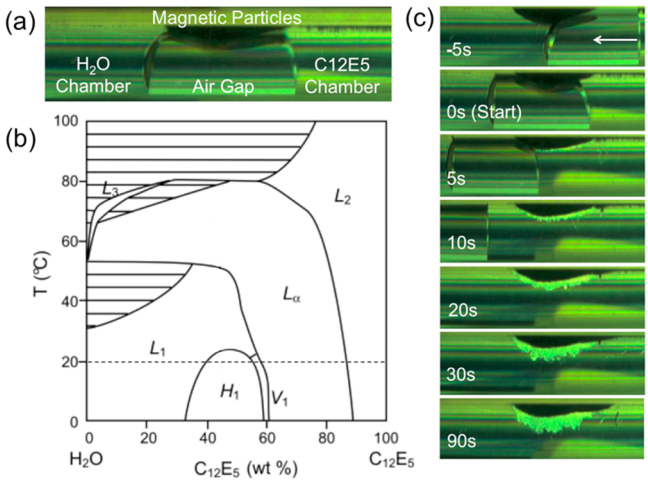


**Figure 8.** (a) Phase change experimental setup. (b) Full phase change plot of water and C12E5. Adapted with permission from ref 14. Copyright 2012 IOP Publishing Ltd. (c) Phase change in device as time varies from 0 to 90 seconds using water and C12E5 surfactant. Liquids are being pumped from right to left at a rate of 0.14 mm/second while the magnetic beads are held in place using an externally applied magnetic field.

phases: $L_1$ and $L_2$, isotropic (micellar); $H_1$, hexagonal; $L_\alpha$, lamellar; and $V_1$, cubic. The hexagonal to $L_1$ transition occurs at 23 °C, which is above the 20 °C temperature at which measurements were performed. The phase change experiments were carried out by first inserting two liquid reservoirs of water (with MBs) and C12E5 into the tube separated by an air gap, as seen in Figure 8a. The MBs were then transported across the air gap into the surfactant reservoir. Photographs of the early stages (from 5 to 90 s) of the resulting phase change are shown in Figure 8c. It is apparent from the photographs that during the dilution of the concentrated surfactant in the reservoir by the water transferred by the MBs a gradient of surfactant concentrations develops, inducing phase transitions into the different liquid crystalline phases present in the dilution path. After 10−20 s, a significant volume of birefringent liquid crystalline phase is observed as the water diffuses out from the MB cluster.

A longer time observation of the dilution process (up to 25 min) is illustrated in Figure 9. As the concentration gradient develops toward a more homogenous state, the volume of liquid crystalline phases also increases and appears colored under cross-polarized microscopy[15] because of a periodic arrangement of the surfactant molecules in the hexagonal or lamellar phase, with dimensions in the range of wavelengths of visible light. The diffusion process continues slowly with time, leading to a homogeneous composition in the test chamber and the disappearance of the liquid crystalline phases, indicating that the equilibrium concentration in the test chamber is still in the initial $L_2$ phase. By replicating the experiment described multiple times, the surfactant concentration in the test chamber can be increased further until equilibration to the single isotropic phase is no longer observed. Counting the number of steps required to achieve such observation allows the determination of the concentration for the $L_2$ to $L_\alpha$ transition. The equilibrium process of each transfer can be accelerated by

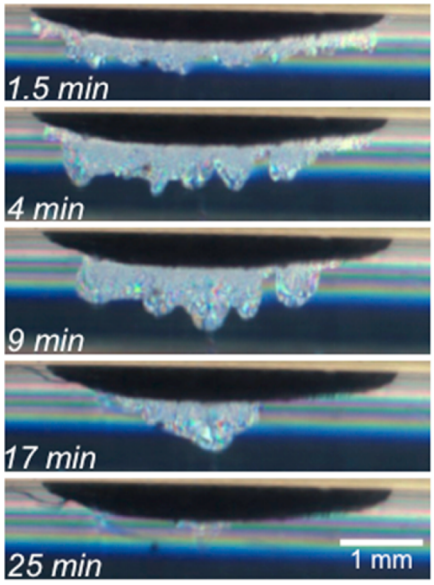


**Figure 9.** Phase change in the device as time varies from 1.5 to 25 min using water and C12E5 surfactant. Liquids are stationary, and the magnetic beads are held in place using an externally applied magnetic field.

physically agitating the volume of liquid. This can be done by alternating magnetic fields on opposite sides of the device using electromagnets or by the utilization of rod-shaped magnets within the device itself.

In order to establish that this method can provide quantitative phase diagram information, an experiment was performed in the vicinity of the $L_1$ to $L_\alpha$ phase transition. The goal of this experiment was to start at the 50% point on the phase diagram seen in Figure 8a at ~25 °C (above the hexagonal phase) and move in the C12E5-rich direction until the $L_\alpha$ phase is reached. The device consisted of a test chamber of 20 $\mu$L containing 50:50 C12E5/$H_2O$ and a 180 $\mu$L reservoir containing pure C12E5 and ~0.2 mg of MBs (corresponding to a carry-over volume of ~0.5 $\mu$L). On the basis of this carry-over volume, the concentration in the test chamber should reach the 56:44 C12E5/$H_2O$ ratio after six transfers. As seen in Figure 10a,b, after six transfers, a uniform phase change from isotropic to lamellar has indeed occurred. This indicates that in this example the accuracy is on the order of ~1% or better of the concentration. This method also allows for a trade-off between accuracy and experiment time by adjusting the mass of the MBs (and corresponding carry-over volume).

To determine the possible effect of liquid being transported along the walls of the tube (rather than by the MB cluster), an experiment identical to the one described above (spanning the transition region between $L_1$ and $L_\alpha$) was performed without MBs. As seen in Figure 10c,d, no phase change was observed in this case. Clearly, the effect of liquid being transported along the walls of the tube is minor at best.

During multiple transports between two fluids, the viscosity of the resulting mixture can change significantly. Therefore, the effect of viscosity on carry-over volume needs to be determined. An experiment was performed comparing the transport using pure water versus 60:40 mixture of water/glycerin. The two fluids have similar surface tensions (73 vs 69 dyn/cm) but quite different viscosities (1 vs 3.7 cP). As shown in Figure 11, the carry-over volume of the two types of fluids is nearly the same in spite of the difference in viscosity. Therefore, the transport between two fluids with different viscosities is not going to affect the results provided by this method.

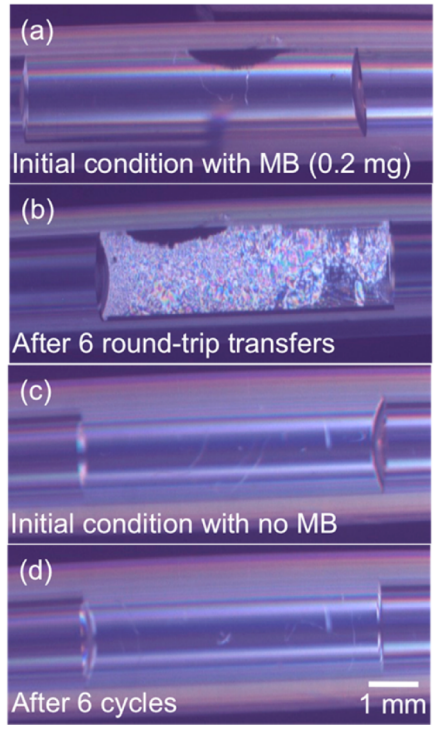


**Figure 10.** Two devices prepared with a test chamber initial concentration of 50:50 C12E5/$H_2O$ and reservoir containing pure C12E5. Using ~0.2 mg beads from initial condition (a) to 6 transfers (b), the sample transitions from L1 to L$\alpha$ phase. In the absence of MBs, no phase change is seen (c, d). Experiment was performed at 25°C.

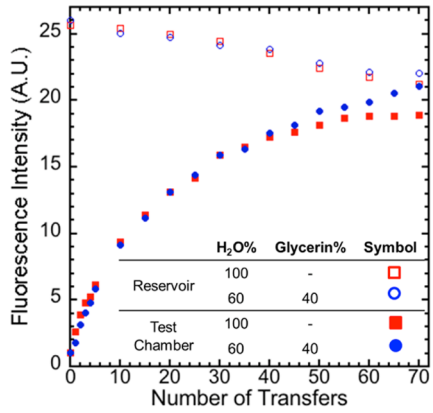


**Figure 11.** Fluorescence intensity as a function of the number of transfers for liquids with similar surface tension and different viscosity: water (73 dyn/cm, 1 cP) and 60:40 $H_2O$/glycerin mixture (69 dyn/cm, 3.7 cP).

## 4. SUMMARY AND CONCLUSIONS

The use of MBs to transport quantifiable liquid volumes (on the microliter scale) between reservoirs in a tube isolated by a surface tension air valve is reported. The MBs were controlled by an external magnetic field, and the liquid reservoirs were translated by a syringe pump. The carry-over liquid volume transported by the MBs was quantified by adding a fluorescent dye in one of the reservoirs and tracking the fluorescent signal after each transfer. The carry-over volume was determined to

be in the range of ∼2 to 3 μL/mg of MBs. This lab-in-tube approach was successfully applied to the exploration of phase changes in mixtures of water and the surfactant C12E5.

It is clear that the methodology proposed is feasible and attractive for the determination of the surfactant phase diagrams when small sample quantities are available and fine resolution on the composition is required. However, the current experimental setup design requires too much time (∼25 min) to achieve complete equilibration in the test chamber. Such equilibration time combined with the transfer volume used would require days for complete phase diagram exploration. This limitation can be overcome by either reducing the diameter of the tube and/or by using magnetic particles as a mini "stir-bar" during the equilibration process. Application of variable magnetic field could induce movement of MBs during the equilibration time, introducing convective mixing that would accelerate the equilibration time, possibly down to a few seconds. Using microfluidic design, multiple parallel experiments (exploring different sections of the phase diagram) could be carried out simultaneously. Another possible extension of this work is the use of small-angle X-ray scattering (SAXS) to characterize the symmetries of the phases and allow a precise discrimination of the different liquid crystal line phases. The lab-in-tube technique can be combined with X-ray scattering analysis in cases where birefringence does not unequivocally discriminate the phase. The device can be placed on the sample stage in the SAXS apparatus, and the measurement can be performed directly on the sample inside the tube without the need of transfer.

## AUTHOR INFORMATION

### Corresponding Author

*E-mail: a.steckl@uc.edu.

### Notes

The authors declare no competing financial interest.

## ACKNOWLEDGMENTS

N.B. was partially supported by a P&G internship.

## REFERENCES

(1) Gijs, M.; Lacharme, F.; Lehmann, U. Microfluidic Applications of Magnetic Particles for Biological Analysis and Catalysis. *Chem. Rev.* **2010**, *110*, 1518−1563.

(2) Kozissnik, B.; Dobson, J. Biomedical Applications of Mesoscale Magnetic Particles. *MRS Bull.* **2013**, *38*, 927−932.

(3) Bordelon, H.; Adams, N.; Klemm, A.; Russ, P.; Williams, J.; Talbot, H.; Wright, D.; Haselton, F. Development of a Low-Resource RNA Extraction Cassette Based on Surface Tension Valves. *ACS Appl. Mater. Interfaces* **2011**, *3*, 2161−2168.

(4) Adams, N.; Creecy, A.; Majors, C.; Wariso, B.; Short, P.; Wright, D.; Haselton, F. Design Criteria for Developing Low-Resource Magnetic Bead Assays Using Surface Tension Valves. *Biomicrofluidics* **2013**, *7*, 14104.

(5) Vitiello, G.; Mangiapia, G.; Romano, E.; Lavorgna, M.; Guido, S.; Guida, V.; Paduano, L.; D'Errico, G. Phase Behavior of the Ternary Aqueous Mixtures of Two Polydisperse Ethoxylated Nonionic Surfactants. *Colloids Surf., A* **2014**, *442*, 16−24.

(6) Lu, J.; Liyanage, P.; Solairaj, S.; Adkins, S.; Arachchilage, G.; Kim, D.; Britton, C.; Weerasooriya, U.; Pope, G. *Recent Technology Developments in Surfactants and Polymers for Enhanced Oil Recovery*, 6th International Petroleum Technology Conference, Beijing, China, March 26−28, 2013.

(7) Ahmad, J.; Amin, S.; Kohli, K.; Mir, S. R. Construction of Pseudoternary Phase Diagram and Its Evaluation: Development of Self-Dispersible Oral Formulation. *Int. J. Drug Dev. Res.* **2013**, *5*, 84−90.

(8) Laughlin, R. *The Aqueous Phase Behavior of Surfactants*; Academic Press: New York, 1996.

(9) Warren, P.; Buchanan, M. Kinetics of Surfactant Dissolution. *Curr. Opin. Colloid Interface Sci.* **2001**, *6*, 287−293.

(10) Laughlin, R.; Lynch, M.; Marcott, C.; Munyon, R.; Marrer, A.; Kochvar, K. Phase Studies by Diffusive Interfacial Transport Using Near-Infrared Analysis for Water (DIT-NIR). *J. Phys. Chem. B* **2000**, *104*, 7354−7362.

(11) Lynch, M.; Kochvar, K.; Burns, J.; Laughlin, R. Aqueous-Phase Behavior and Cubic Phase-Containing Emulsions in the C12E5-Water System. *Langmuir* **2000**, *16*, 3537−3542.

(12) Leng, J.; Joanicot, M.; Ajdari, A. Microfluidic Exploration of the Phase Diagram of a Surfactant/Water Binary System. *Langmuir* **2007**, *23*, 2315−7.

(13) Shim, J.; Cristobal, G.; Link, D.; Thorsen, T.; Jia, Y.; Piattelli, K.; Fraden, S. Control and Measurement of the Phase Behavior of Aqueous Solutions Using Microfluidics. *J. Am. Chem. Soc.* **2007**, *129*, 8825−35.

(14) Hishida, M.; Tanaka, K. Transition of the Hydration State of a Surfactant Accompanying Structural Transitions of Self-Assembled Aggregates. *J. Phys.: Condens. Matter* **2012**, *24*, 284113.

(15) Strey, R.; Schomacker, R.; Roux, D.; Nallet, F.; Olsson, U. Dilute Lamellar and L3 Phases in the Binary Water-C12E5 System. *J. Chem. Soc., Faraday Trans.* **1990**, *86*, 2253−2261.